Numerical simulation of heterogeneous phase transformations

H. Combeau, J. Lacaze

JOURNAL DE PHYSIQUE IV
Colloque C7, supplément au Journal de Physique III, Volume 3, novembre 1993

Numerical simulation of heterogeneous phase transformations

H. COMBEAU and J. LACAZE

LSG2M, URA 159 du CNRS, Ecole des Mines, 54042 Nancy cedex, France

ABSTRACT
A numerical model is presented for the simulation of diffusion controlled phase transformations in multicomponent alloys. A closed system is considered, with simple geometric shape, either planar, cylindrical or spherical. The temperature inside this microscopic volume is homogeneous, but can vary according to any specified monoteneous law. Particular care has been given to the description of the solute profiles where the concentration gradients are the steepest, i.e. near the interface between the parent and the resultant phases. Solute redistribution at the interface is described by means of an original method which ensures that the overall solute balance is satisfied. A non linear system is obtained which includes the diffusion equations in both phases and the boundary conditions. The solution of this system makes use of a special algorithm which has been devised for a quick convergence. An example is presented which deals with microsegregation build-up during solidification of a multi-component nickel base alloy.

INTRODUCTION
Numerous numerical models have been proposed in the literature to describe diffusion controlled phase transformations in binary alloys, while only a limited number has been devised to treat multicomponent alloys. This is particularly true in the field of solidification where the few works which can be cited have put emphasis on diffusion in the solid phase [1-3]. In fact, experimental knowledge of microsegregation build-up during solidification has shown that limited liquid diffusion might be of some importance on the solute distribution at the end of solidification [4,5]. The present work was undertaken in this line of study, with the aim at investigating the effect of limited diffusion in both solid and liquid phases at the scale of the solidification microstructure. The numerical model which is proposed is however of a general purpose and could be used for any other diffusion controlled transformation. An example is presented which deals with microsegregation build-up during solidification of a multi-component nickel base alloy.

NUMERICAL MODEL
The phase transformation is to be described in a system which is closed with respect to exchange of matter, and it is assumed that solute transport in the parent and precipitated phases is only due to volume diffusion. The system is defined as a microscopic volume element with a size L related to the solidification microstructure; it has a simple geometric shape, either planar, cylindrical or spherical. The microscopic volume element is centred on the first nucleus of the precipitated phase, and the transformation proceeds with an interface homothetic to the shape of the system. Diffusion of any solute i is thus monodirectional and obeys the following equation, where the space coordinate is noted x :

$$\frac{\partial w_i^{\phi}}{\partial t} = \nabla \left(D_i^{\phi} \nabla w_i^{\phi} \right) \qquad (1)$$

with $\frac{\partial w_i^{s}}{\partial x} = 0$ at x=0 and $\frac{\partial w_i^{l}}{\partial x} = 0$ at x=L

where ϕ denotes either the parent liquid phase, superscript l, or the precipitated solid phase, superscript s, and $^{\circ}w_i$ is the nominal content of the alloy in solute i.

Local thermodynamic equilibrium is assumed at the interface and may be expressed by the equation which relates the liquidus temperature of the liquid at the interface to its composition and the equation which

describes solute partitioning between the two phases. While any kind of relations could have been introduced in the algorithm, the very simple following equations have been used :

$$T = T_m + \sum_i m_i w_i^{l*} \qquad (2)$$

$$w_i^{s*} = k_i w_i^{l*} \qquad (3)$$

where $w_i^{\phi*}$ is the i content in phase ϕ at the interface, T is the liquidus temperature corresponding to the liquid composition at the interface, T_m is the fusion temperature of the pure solvent, m_i is the liquidus slope related to solute i and k_i is the so-called partition coefficient of solute i.

Equations 1 to 3 define a non-linear problem which involves a moving interface with variable composition and occasionally steep compositional gradients. To solve it, the present work makes use of the "finite volume method" [6] with a particular algorithm in order to track the interface location. Once the time has been incremented by a fixed value Δt, and the new temperature determined, an iterative procedure is followed during which are performed, successively, meshing, calculation of the composition at each new mesh point, resolution of the diffusion equations and determination of the new position and composition of the interface.

The mesh is changed at each time step all along the transformation so as to maintain the interface at a boundary between two cells. The number of mesh points on both sides of the interface is allowed to vary, while the total number of mesh points, N, is constant. Each time the meshing procedure is used, the number of mesh points to the left side of the interface, N_S, is first calculated as $N_S=[\xi\,(L)^{-1}N]+1$, where ξ is the interface position. The number of mesh points to the right side of the interface, N_I, is thus $N_I=N-N_S-1$, while the point corresponding to the interface is given the number N_S+1. The indices have been chosen with respect to the phases, solid to the left hand and liquid to the right hand of the interface. In each of the domains, the size of the mesh volumes, $\Delta x(j)$ for the cell numbered j, was calculated according to a geometric progression such that the finest cells are those close to the interface. A mesh point is implemented at the centre of each mesh volume, with right and left neighbour points designated East and West respectively. The distance between the j^{th} mesh point and its first neighbours are accordingly denoted $\delta x_w(j)$ and $\delta x_e(j)$. The point related to the interface has a zero size and volume because it is used only to compute the composition at the interface as described below. The volume of each cell j, V(j), as well as the areas of its two limiting surfaces, $S_w(j)$ and $S_e(j)$, were calculated according to the specified geometry, planar, cylindrical or spherical. The final shape of the meshing obtained by this procedure is illustrated in figure 1, where the dotted lines are the boundaries between two neighbouring mesh volumes.

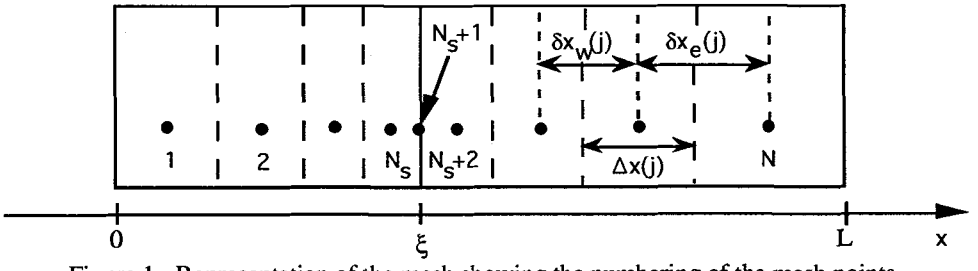

Figure 1 - Representation of the mesh showing the numbering of the mesh points.

Redistribution of solutes from a old to a new mesh must be made with some care in order to ensure solute conservation. The corresponding procedure is illustrated in figure 2 for the cells close to the interface. In this figure, ξ^0 and ξ^1 are respectively the position of the interface at time t, which is known, and at time $t+\Delta t$, which is looked for by successive iterations. The corresponding solute profile is shown in plain lines for ξ^0 and bold lines for ξ^1. As the interface moves from its initial to its new position, there is solute partitioning between the solid and liquid phases. Solute conservation at the interface is written as :

$$\int_t^{t+\Delta t} S^\xi \frac{d\xi}{dt} (w_i^{l*} - w_i^{s*})\, dt = \int_t^{t+\Delta t} \left[- D_i^l \frac{\partial w}{\partial x}\Big|^{s*} + D_i^s \frac{\partial w}{\partial x}\Big|^{l*} \right] S^\xi\, dt \qquad (4)$$

where $w_i^{\phi*}$ and $\frac{\partial w}{\partial x}|^{\phi*}$ are respectively the content and the gradient in solute i at the interface in phase ϕ, either solid s or liquid l, and D_i^{ϕ} is the diffusion coefficient of solute i in phase ϕ. S^{ξ} is the area of the interface, the value of which changes with the displacement for cylindrical and spherical geometries.

It is assumed that the composition and solute gradients at the interface do not change when the interface moves from ξ^0 to ξ^1 during the time step Δt. Taking into account equation (3), and noting $^{\circ}w_i^{l*}$ the composition of the liquid at the interface at time t, equation (4) can be simplified to give :

$$^{\circ}w_i^{l*} (1 - k_i) \int S^{\xi} \frac{d\xi}{dt} dt = \left[- D_i^l \frac{\partial w}{\partial x}|^{l*} + D_i^s \frac{\partial w}{\partial x}|^{s*} \right] \int S^{\xi} dt \qquad (5)$$

The left hand side of equation (5) is the amount of solute rejected when k_i is less than 1, absorbed when k_i is more than 1, by the solid during its growth between ξ^0 and ξ^1. It is used as a source term at the interface. The discretized version of equation (5) is then written :

$$^{\circ}w(i;N_s+1) (1 - k_i) V^* = \left[D_i^s \frac{k_i w(i;N_s+1) - w(i;N_s)}{\delta x_w(N_s+1)} - D_i^l \frac{w(i;N_s+2) - w(i;N_s+1)}{\delta x_e(N_s+1)} \right] S^* \Delta t \qquad (6)$$

where $^{\circ}w(i;N_s+1)$ is the composition of the liquid at the interface at time t and w(i;j) is the i content in the j^{th} mesh volume at time $t+\Delta t$; $S^* = \frac{1}{\Delta t} \int S^{\xi} dt$ and $V^* = \int S^{\xi} \frac{d\xi}{dt} dt$.

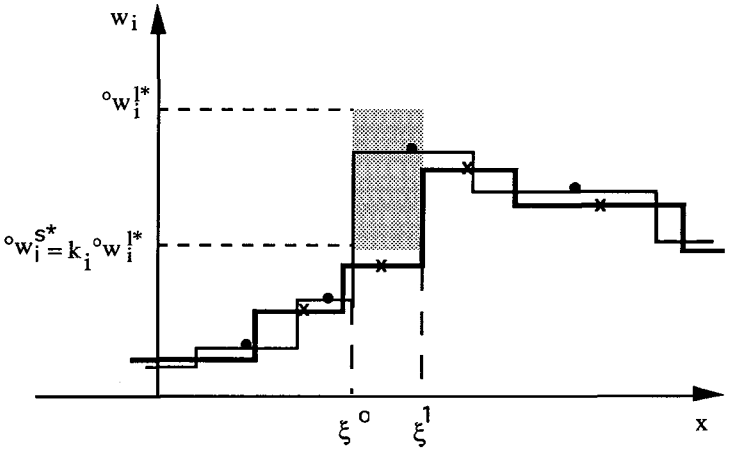

Figure 2 - Schematic representation of solute profile before (plain lines) and after (bold lines) remeshing for cells close to the interface. At time t, before remeshing, the interface is at ξ^0, it moves at position ξ^1 at time $t+\Delta t$ where the new mesh is calculated. Circles and crosses indicate the cell centres in the corresponding mesh. The shaded area represents the source term in equation (6).

According to the finite volume discretization [6], the single phase diffusion equation is written for each solute i and in each point j, other than N_s+1, as :

$$V(j) \frac{\Delta w(i;j)}{\Delta t} = D_i^{\phi} \left\{ S_e(j) \frac{w(i;j+1) - w(i;j)}{\delta x_e(j)} - S_w(j) \frac{w(i;j) - w(i;j-1)}{\delta x_w(j)} \right\} \qquad (7)$$

where $\Delta w(i;j) = w(i;j) - {}^{\circ}w(i;j)$ is the change of w(i;j) during Δt.

The solution of the above set of equations is found by means of the TDMA algorithm [6]. The temperature calculated from the new liquid composition at the interface, T^{ξ}, is calculated by inserting the $w(i;N_s+1)$ values in equation (2). It should be equal to the specified temperature at time $t+\Delta t$, $T^{t+\Delta t}$. The difference

between these two temperatures, $\Delta T^{t+\Delta t}$, is calculated and the ratio $\frac{\Delta T^{t+\Delta t}}{T^{t+\Delta t}}$ is compared to a convergence criteria, typically set equal to 10^{-10}. In case the ratio is higher than this value, a better estimate of the interface position is calculated by means of the Newton method.The procedure giving the position of the interface is then followed again until convergence has been obtained. Once this is achieved, and after reinitialization of the data, the time is incremented and the whole procedure is repeated.

VALIDATION OF THE NUMERICAL MODEL

The soundness of the model has first been checked with input data expected to give either the lever rule or the Gulliver-Scheil predictions. The former is related with infinitely fast diffusion in both the solid and liquid phases, while the latter corresponds to rapid diffusion in the liquid phase and no diffusion in the solid phase. In the case of fast diffusion, the diffusion coefficient was put equal to 10^{-3} m^2s^{-1}, and for low diffusion to 10^{-16} m^2s^{-1}. The partition coefficient, the liquidus slope and the nominal solute content were respectively taken equal to 0.5, -10.0 K.(wt pct)$^{-1}$ and 1.0 wt pct. A planar geometry with a volume element 100 μm in length and a 10.0 Ks^{-1} cooling rate were considered. Calculations were performed up to a solid fraction equal to 0.95, and a very good agreement was obtained for the two limiting cases. As an example, figure 3 compares the prediction of the Gulliver-Scheil model, shown with the bold interrupted line, and the numerical calculation plotted with the superimposed continuous line. In addition, the calculated solute profiles along the length of the volume element, at partial solidification time 0.5 s, 2.0 s and 10.0 s, have been plotted and show that the liquid composition is actually homogeneous at any stage of the solidification.

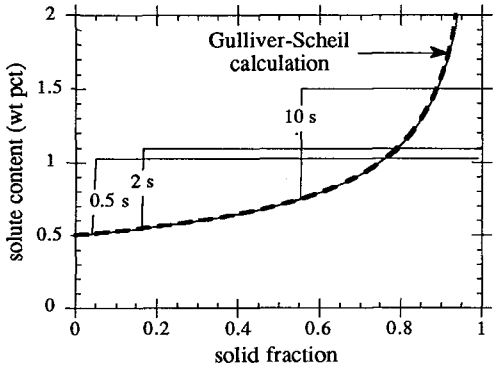

Figure 3 - Comparison of the calculated evolution of the composition at the interface with the predictions of the Gulliver-Scheil model. The solute distribution profile at three partial solidification times is also shown.

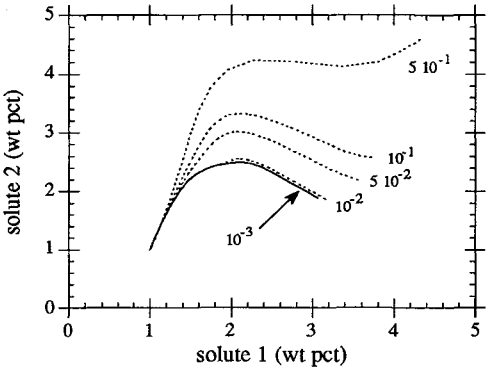

Figure 4 - Effect of the time step upon the solidification path calculated for a ternary alloy with solutes having the same properties except for the liquid diffusion coefficient.

In the above calculation, the possible effects arising from the discretization in time and space are certainly related to each other. However, for a time step equal to 0.1 s, no difference was found between results obtained with 50 and 200 mesh points. To further check the possibilities of the code, a second set of calculations were performed in the case of a ternary alloy with equivalent solutes except for their liquid diffusion coefficient. The partition coefficient and liquidus slope of solute 1 and 2 were as above, their diffusion coefficient in the solid were both equal to 10^{-14} m^2s^{-1}, while their liquid diffusion coefficient were respectively 10^{-9} m^2s^{-1} and 10^{-10} m^2s^{-1} for solute 1 and solute 2. Calculations have been made for a planar geometry with a microscopic volume element 100 μm in length, with 200 mesh points. While the overall solute contents are in any case verified, a very strong effect of the time step was found, as illustrated in figure 4 where the so-called solidification path, i.e. the locus of the point representing the liquid composition at the interface, is plotted in the composition plane for time step varying from 10^{-3} s to 5.0 10^{-1} s. In the present case which was calculated for a cooling rate equal to -10.0 $K.s^{-1}$, it was thus noted that the time step should be 10^{-2} s or less. This effect might be due to the fact that the steep composition gradient associated with the low diffusion rate of the second solute is very sensitive to the growth rate of the interface; a small time step is thus needed to accurately describe its evolution.

The very particular shape of the solidification path which was obtained is related to the difference in the liquid diffusion coefficient : the lower its value, the higher the solute build-up ahead of the solid-liquid interface at the solidification beginning. After a while, the boundary layer for the slow diffusing species stabilizes and the corresponding solute content changes much more slowly. This is like the steady-state solute distribution during crystal growth, where the solid which deposits has a composition equal to that of the liquid far away from the interface. In the present case however, the composition at the interface of the fast diffusing species still increases, leading to a dramatic change of the slope of the solidification path. The calculation has been made for various cooling rates, as illustrated in figure 5. When the cooling rate is decreased, there is more time for diffusion to proceed, so that the difference in the solute build-up of the two solutes is progressively limited to the very beginning of the solidification and smoothed out. On the figure, the reference curve is the one calculated with the Gulliver-Scheil model.

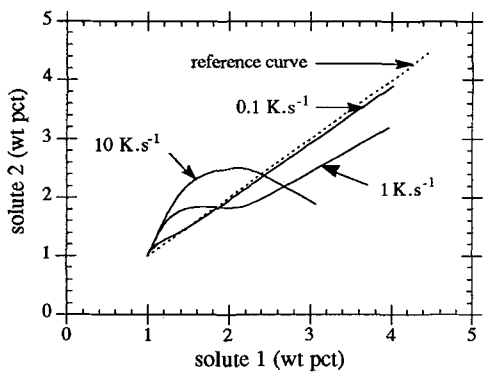

Figure 5 - Solidification path for a ternary alloy with identical solutes except for their diffusion coefficient in the liquid. Calculations have been made up to a fraction of solid equal to 0.95, for various cooling rates which are indicated on the figure. The curves may be compared to the reference curve calculated when the liquid is assumed to be chemically homogeneous at any temperature.

MICROSEGREGATION IN A NICKEL-BASE SUPERALLOY

Experimental determination of microsegregation in a nickel-base superalloy has been made by means of an automatic micro-probe analyser on different sections of an as-cast single-grain grown at 4.0 10^{-3} m.s^{-1} under a temperature gradient of 3000 K.m^{-1}, i.e. corresponding to an average cooling rate equal to 0.2 K.s^{-1}. The experimental method and the main results have been previously described [7,8]. The solidification microstructure was characterized by the density of primary axes, which was in the range of 10.0 mm^{-2}; a cylindrical volume element was thus assumed, with a radius L=175.0 10^{-6} m. Table I lists the input data used for the calculations. The nominal solute contents (wt pct) are the average values obtained from microprobe analysis; the partition coefficients are from an earlier experimental determination [9], except for W which is here set equal to 1.6; the liquidus slopes (K.pct^{-1}) are those given by Cook and Guthrie [10] in the case of alloy IN100 and from the binary diagrams for solutes absent in this alloy; the solid-state diffusion data, D_i^0 (m^2s^{-1}) and $\frac{Q_i}{R}$ (K), are mainly values for binary alloys taken from Smithells [11]. All the liquid diffusion coefficients were put equal to 1.0 10^{-9} m^2s^{-1}. Knowing the solidification interval of AM1 alloy, which has a liquidus equal to 1365 °C and a eutectic reaction at 1315 °C, the liquidus slopes given in table I were found to be far too large, probably due to the well-known flattening of the liquidus surface near the eutectic reaction. They have thus been all multiplied by 0.53 so as to give a eutectic fraction of 0.05 according to the Gulliver-Scheil model; this led to T_m=1423.5 °C.

The calculated solute profiles for Ta, Ti and W are shown in full lines in figure 6-a, where they are compared with the experimental profiles shown dotted. The agreement is rather good, and could be better if solid-state diffusion after solidification completion would had described. In fact, the Gulliver-Scheil model gives results which are not far from the present calculations. However, a particular feature is well described by the present simulation which could not be reproduced by the Gulliver-Scheil model; this is the inverted curvature at low solid fraction which is related to limited liquid-state diffusion during the lateral development of the solidification microstructure. This is illustrated in figure 6-b which presents the data of figure 6-a related to W at low solid-fraction, and compares them to the Scheil-Gulliver calculations. This effect, which is now well-known on an experimental basis, has rarely been emphasized in the literature, while it might clearly affect the final solute distribution at the scale of the microstructure.

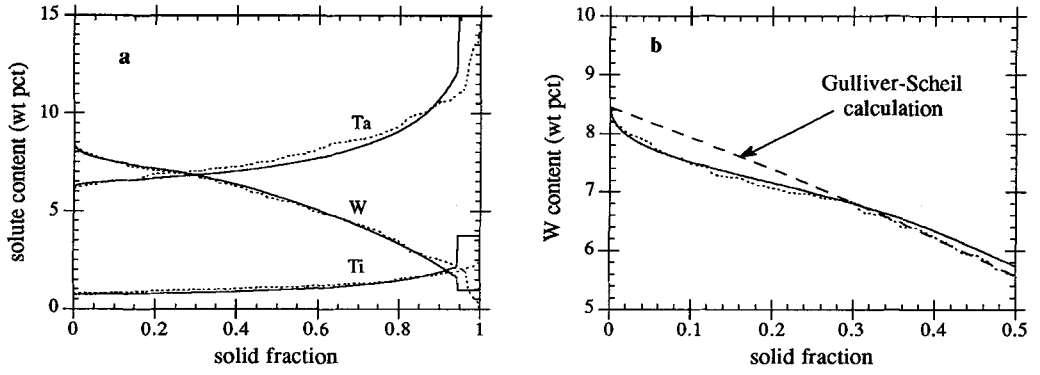

Figure 6 - **a** : Comparison of calculated (full lines) and experimental (dotted lines) solute profiles of Ta, Ti and W measured on a nickel-base as-cast single grain. **b** : Enlargement of the curves shown in fig. 6-a for W and comparison with the prediction according to the Gulliver-Scheil model.

element	Al	Co	Cr	Mo	Ta	Ti	W
nominal content	5.02	6.455	7.28	1.89	8.17	1.22	5.28
partition coefficient	0.91	1.09	0.92	0.78	0.76	0.58	1.6
liquidus slope	- 11.25	0.525	- 2.25	- 3.6	- 3.75	- 12	0.6
D_i^o	$1.87\ 10^{-4}$	$2.77\ 10^{-4}$	$8.52\ 10^{-4}$	$3.0\ 10^{-4}$	$2.05\ 10^{-4}$	$0.86\ 10^{-4}$	$2.87\ 10^{-4}$
$\frac{Q_i}{R}$	$3.22\ 10^6$	$3.43\ 10^6$	$3.51\ 10^6$	$3.42\ 10^6$	$3.59\ 10^6$	$3.09\ 10^6$	$3.96\ 10^6$

Table I - Input data for the alloying elements of nickel-base AM1 superalloy

SUMMARY

A numerical model for the simulation of diffusion controlled phase transformations in multicomponent alloys has been presented. This model has first been validated against analytical solutions for solidification of binary alloys. Then, the influence of limited diffusion of solutes in the liquid phase has been emphasized in the case of ternary alloys. Finally, a comparison of calculated and experimental results related to microsegregation in a multicomponent nickel-base alloy was undertaken. It showed a satisfactory agreement concerning the solute distribution, in particular at low solid fraction where is observed a change in sign of the curvature of the solute profile with respect to the predictions made with the Gulliver-Scheil model.

ACKNOWLEDGMENTS

This study has been partly supported by the French scientific program "Microstructure et Propriétés des Superalliages Monocristallins". The authors are indebted to R. Tintiller from SNECMA for providing the AM1 single grain parts, and to N. Siredey who has carried out the micro-probe study; they wish to thank V. Trublin and A.-V. Ventre who have implemented the algorithm as a project during their studies at the Ecole des Mines de Nancy.

REFERENCES

[1] Ueshima Y., Mizoguchi S., Matsumiya T. and Kajioka H. : *Metall. Trans.* **17B**(1986)845
[2] Roosz A. and Exner H.E. : *Acta Metall. Mater.* **38**(1990)375
[3] Mietinnen J. : *Metall. Trans.* **23A**(1992)1155
[4] Lacaze J. and Lesoult G. : in "Nature and Properties of Semi-Solid Materials", TMS (1991)105
[5] Lacaze J. and Lesoult G. : to appear in Materials Science and Engineering A
[6] Patankar S.V. : Numerical Heat Transfer and Fluid Flow, Hemisphere, Washington DC, 1980
[7] Siredey N : Thesis, INPL, Nancy, France, 1991
[8] Siredey N. and Lacaze J. : 1992 Vacuum Metallurgy Conference, *Le Vide, Les Couches Minces* **261**(1992)149
[9] Chehaibou A. : Thesis, INPL, Nancy, France, 1988
[10] Cook R.M. and Guthrie A.M. : *Foundry Trade J.* (1966)686
[11] Smithells : Metals Reference Handbook, Butterworths, 3rd Edition, 1962